CARBON 50 (2012) 2845–2852

Available at www.sciencedirect.com

SciVerse ScienceDirect

journal homepage: www.elsevier.com/locate/carbon

Investment casting of carbon tubular structures

Longbing He [a], *Tao Xu* [a], *Jun Sun* [a], *Kuibo Yin* [a], *Xiao Xie* [a], *Liang Ding* [b], *Helen Xiu* [c], *Litao Sun* [a,*]

[a] *SEU-FEI Nano-Pico Center, Key Lab of MEMS of Ministry of Education, Southeast University, Nanjing, 210096, PR China*
[b] *Key Lab for Power Machinery and Engineering of Ministry of Education, Shanghai Jiao Tong University, Shanghai, 200240, PR China*
[c] *FEI Company, Shanghai Nanoport, No. 690 Bibo Road, Shanghai, 201203, PR China*

ARTICLE INFO

Article history:
Received 6 December 2011
Accepted 17 February 2012
Available online 24 February 2012

ABSTRACT

Carbon tubular structures (CTSs) were prepared using metal nanowires/nanotubes, either Ag or Te, as templates. The CTSs are formed by electron beam-induced carbon deposition on the nanowires/nanotubes and the subsequent removal of the core material by direct heating or Joule heating. We call this process "investment casting" of CTSs. The length of the fabricated CTSs varies from sub-micron to tens of microns, while the diameter and wall-thickness may vary from less than ten nanometers to over a hundred nanometers and few nanometers to tens of nanometers, respectively. These parameters can be controlled by the templates and the carbon deposition. With Te nanotubes as templates, it is possible to form tube-in-tube hollow CTSs. By designed construction of Ag nanowires, various CTS-based seamless structures can also be obtained. Through thermal annealing or Joule heating, the amorphous CTSs can be converted to graphitized structures, which show excellent mechanical performance on nano-manipulation. The technique provides a new method of constructing carbon-based complex and multifunctional structures.

1. Introduction

Carbon tubular structures (CTSs), such as carbon nanotubes (CNTs) [1], have dramatically shown prospective advantages in design and fabrication of future micro-/nano-electromechanical systems [2,3], nanofluidic devices [4–6], nanopipettes [7], nanosensors [8,9] and nanoactuators [10]. Especially in biomedical and micro-/nano-fluidics, CTSs could provide much smaller channels with superior mechanical and thermal properties than those fabricated by lithography or nanoimprint method, which benefit the integration of bio-chips and can highly promote potential applications such as DNA analysis [11], polymerase chain reaction, drug delivery [12,13] and capillary electrophoresis [14]. To accomplish these potential applications, two vital techniques are generally prerequisite. One is the fabrication of CTSs with desirable geometry including diameter, length, and wall thickness; the other is the precise processing of the CTSs through cutting, peeling and especially seamless welding for nanochannels [15–21]. For commercial CNTs, although diverse approaches, *e.g.*, arc discharge, laser ablation and chemical vapor deposition can prepare various high-quality multiwall carbon nanotubes (MWCNTs) [22], there are still great challenges in precisely controlling the growth of CNTs with defined diameter and length as well as separating specific nanotubes for specified applications. Meanwhile, the lack of proper techniques to freely manipulate CNTs and implement post-processing of synthesized CNTs in nanoscale also slows down the application process in nanofluidics and nanodevices. Therefore, a delicate method with which CTSs can be fabricated in precise control is still in demand.

Comparing to bottom-up techniques, top-down approaches usually present better compatibility and are easy to integrate with device fabrication. The template approach

* *Corresponding author:* Fax: +86 25 83792939.
E-mail address: slt@seu.edu.cn (L. Sun).
0008-6223/$ - see front matter
doi:10.1016/j.carbon.2012.02.051

provides a feasible way to design diverse tubular structures [23]. Through casting sheath materials on nanowires as cores, robust nanotubes with uniform inner diameters can be obtained by selective etching of the core nanowires [24–28]. The sheath materials can be formed by several state-of-art techniques, including epitaxial growth and vapor phase deposition. However, the existed deposition and etching processes still face problems in precise welding and nanodevice design. The condition of the etching process is also harsh due to the selectivity of the removal of core material without destroying sheath material. Toward all-carbon devices, delicate nanoforming process such as investment casting is required. Particularly, for characterization of structure related electrical and mechanical properties, fabrication of desirable CTSs for the design of prototype nanodevice has shown significant importance. We here present a convenient approach for controllable fabrication of diverse CTSs on demand and CTS-based seamless architectures using well prepared nanowires as templates. Our fabrication and processing assay can highly facilitate nanodevice fabrication and characterization.

2. Experimental

Ag and Te nanowires were purposely selected as templates since they could be well synthesized with featured structures [29–31] and extracted away by direct thermal heating or Joule heating. CTSs were fabricated by electron beam-induced carbon deposition [32] on the template nanowires inside a transmission electron microscope (TEM, Tecnai G20, 200 kV). After carbon deposition, the nanowire templates were subsequently melted and extracted by heating. Direct thermal heating of the template nanowires were conducted with Gatan^{TM} 628 heating holder (0-1300 °C). Manipulation and Joule heating of the template nanowires were performed on Nanofactory piezo-driven scanning tunneling microscopy-transmission electron microscopy (STM-TEM) work platform.

The Ag/Te nanowires were transferred to a copper gird (1000 meshes) and then put into the TEM chamber. During carbon deposition, the electron beam was operated on spot size 6 and spread to cover the template region of interest. Generally, the carbon deposition rate was comprehensively

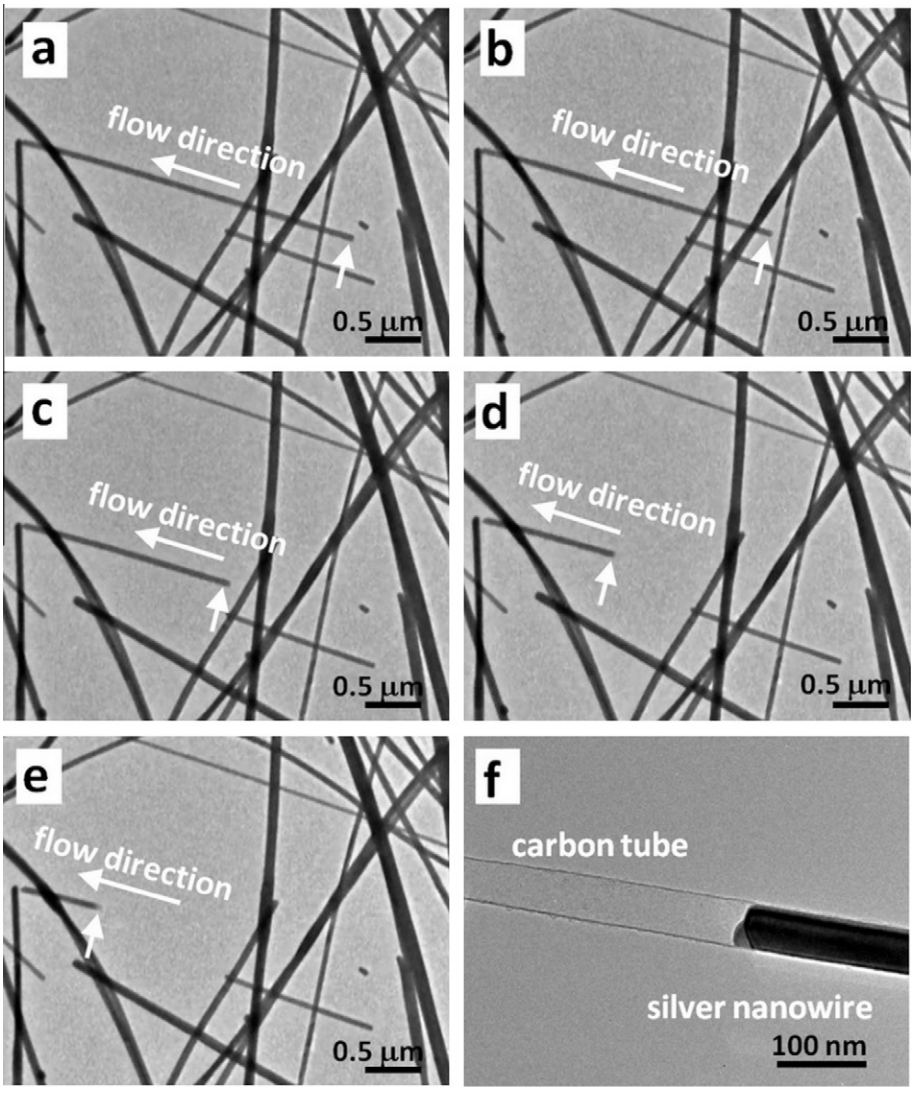

Fig. 1 – (a–e) A typical image sequence of extracting a molten Ag nanowire to form a CTS by heating the copper grid to 560 °C. (f) A snapshot of the intermediate state during extraction of the template Ag nanowire.

determined by spot size, irradiation area of the electron beam, vacuum condition of the column and surface condition of the template (molecular adsorption) [33]. In this experiment, the rate of carbon deposition estimated roughly from a charge coupled device was 0.4 nm/min for the spread electron beam operated on spot size 6 (the irradiation region was approximately 200 μm^2, column vacuum 1.3×10^{-5} Pa). For a convergent electron beam operated on spot size 9 (the irradiation region was approximately 0.03 μm^2, column vacuum 1.3×10^{-5} Pa), the rate of carbon deposition was estimated to be 15 nm/min. By using inducement of Joule heating, the template nanowires were first transferred onto another 1000-mesh copper grid and then the grid was cut into small pieces and one piece was attached onto a gold wire with conductive silver paste as one electrode. The counter-electrode was a MWCNT-decorated tungsten tip fixed onto the piezotube.

3. Results and discussion

Fig. 1 shows a typical image series of the formation of CTSs by extracting the molten template Ag nanowires through heating the stage to 560 °C (see Supplementary video S1). As indicated by the arrow, the molten Ag continuously flows from one end to the other due to surface tension. As the melting point of the Ag nanowires is related to their diameters and surface conditions [34], an elevated temperature is therefore needed to melt all the template Ag nanowires. Besides, the contact conditions between the Ag nanowires and the copper

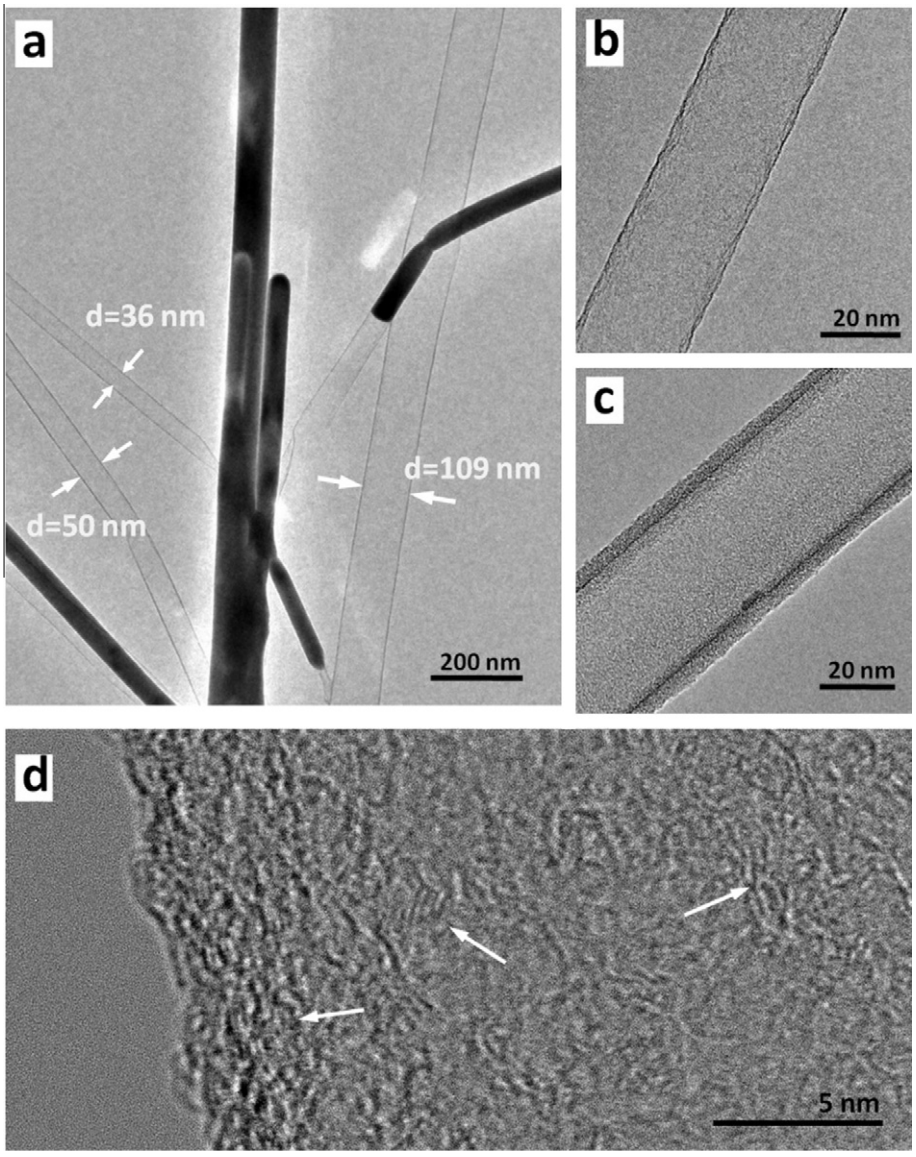

Fig. 2 – (a) CTSs with diverse lengths and diameters. The lengths and diameters of the CTSs are well controlled by the template Ag nanowires. (b) A thin-shell CTS with wall-thickness of approximately 2.3 nm. (c) A thick-shell CTS with wall-thickness of approximately 6.7 nm. (d) High resolution image of the graphitized carbon shell. The arrows indicate graphite structures after extraction of the Ag nanowires at higher temperature (700 °C).

gird affect the thermal conduction, thus the molten Ag nanowires usually flow away in sequence. When the molten Ag has been drained away, a uniform CTS is left behind as shown in Fig. 1(f). The inner diameter of the CTS retains the size of the dimension of the template Ag nanowires without any collapse. Therefore, diverse CTSs can be fabricated through different featured Ag nanowire templates. For Te nanowires, the melting point is much lower and CTSs can be formed by evaporation of the Te core at approximately 300 °C.

Fig. 2(a) shows the CTSs that have been obtained with distinct structural features. Benefiting from the high-quality template Ag nanowires, the formed CTSs are generally uniform and straight with lengths from several microns to tens of microns. The diameters of the CTSs vary from tens of nanometers to more than a hundred nanometers, depending on the template Ag nanowires being used. The wall-thicknesses of the CTSs can be controlled by carbon deposition mass. As shown in Fig. 2(b) for a short irradiation period with a spread electron beam (6 min with spot size 6), the wall thickness of the formed CTS is around 2.3 nm. With longer irradiation time (16 min with spot size 6), the wall thickness significantly increases to 6.7 nm, which is a typical thick nanotube as shown in Fig. 2(c). Although the deposition rate of carbon can be roughly calculated, it is still necessary to monitor the carbon growth to precisely control the wall-thickness of the CTSs since the process of carbon deposition is complex and affected by several factors [33]. The structures of the as-deposited nanotubes are generally amorphous. However, extraction of the core template by heating usually accompanies with thermal annealing of the sheath material. As shown in Fig. 2(d), the CTS formed with a Ag nanowire as template is partial graphitized after extraction of the Ag nanowires, indicating that relative high temperature could significantly improve the crystalline quality of the formed CTSs.

Smaller CTSs can be fabricated by using Te nanowires as templates. Fig. 3(a) and (b) show diverse CTSs fabricated by evaporation of Te nanowires at 300 °C after electron beam-induced carbon deposition. The diameter of the CTSs can scale down to less than 10 nm with proper templates. The formed CTSs are completely amorphous since the temperature used to evaporate the Te templates is rather low. To obtain well graphitized CTSs, post-processing is necessary, such as thermal annealing and catalyst induced structure reconstruction [33,35,36]. For tubular Te templates, tube-in-tube CTSs can also be fabricated as shown in Fig. 3(c). These co-axial hollow nanotubes might provide ideal reaction channels/cells for nanoscale mixing and liquid reactions [37,38]. Besides, the

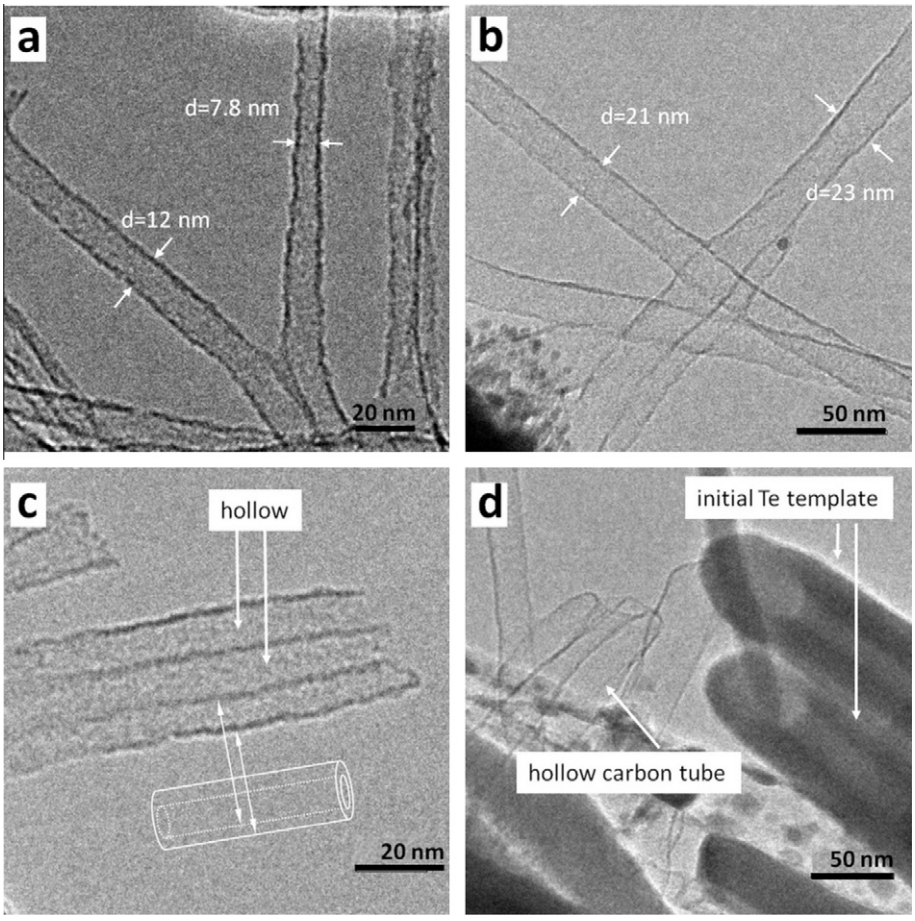

Fig. 3 – Formation of thin CTSs with Te nanowires/nanotubes as templates. The diameters of the fabricated CTSs are around ten nanometers in (a) and twenty nanometers in (b). (c–d) Fabricated tube-in-tube CTSs with Te nanotubes as templates.

formation of these tube-in-tube CTSs demonstrates that the deposited carbon should be generated by decomposition of the hydrocarbon molecules which can diffuse and migrate inside the Te nanotubules. Fig. 3(d) shows the intermediate state of the evaporation process of the Te templates. The newly formed tube-in-tube CTS exactly retains the shape of the tubular Te template, indicating the high accuracy of the aforementioned nano-forming process.

CTSs are ideal for constructing nanodevices due to their highly uniform characteristics and designable geometries. As for nanoscale capillary reactors or nanofluidic channels, precise welding with a seamless joint is critical to the device function and performance. For CNTs, it is still difficult to seal them in atomic scale without blocking the channels especially for cross connections [17,19–21]. However, CTSs fabricated by the method "investment casting" presented here using nanowires as templates sheds light on such issues. Fig. 4 shows some fabricated seamless connections with contacted Ag nanowires as templates schematically presented in the insets. The Ag nanowires are constructed by STM-TEM platform and subsequently transferred to the heating holder. For a head-to-head connection shown in Fig. 4(a), the deposited carbon obviously sealed the joint and formed a continuous nanochannel. The seamless joint should present better mechanical properties than post-welded conjunctions because the connection part is formed simultaneously with the CTSs and show high integrity. For Y-shape and X-shape connections as shown in Fig. 4(b) and (c) respectively, continuous conduits are formed by removing the template Ag nanowires. Even for a more complex structure as shown in Fig. 4(d), the template approach is still capable of constructing multiple nanofluidic channels. Note that the joints usually have spatial structures rather than planar structures due to the overlapping of the template Ag nanowires except for some head-to-head connections. The orifices of the conjunctions are determined by the contact area of the contacted Ag nanowires.

Joule heating can also be applied to extract the metallic core nanowires to fabricate CTSs. A large current is usually needed in order to drain away the Ag nanowires covered by amorphous carbon shell, due to the superheating effect [39]. Meanwhile, some other effects such as electromigration [40] and thermalmigration [41] also play important roles on the formation of CTSs. Fig. 5(a) shows the extraction of Ag under a large bias. The Joule heat abruptly drains away the Ag nanowire by evaporation or electromigration. As can be seen, Joule heating is usually much more drastic than direct thermal heating; therefore the formed CTS is accompanied with some

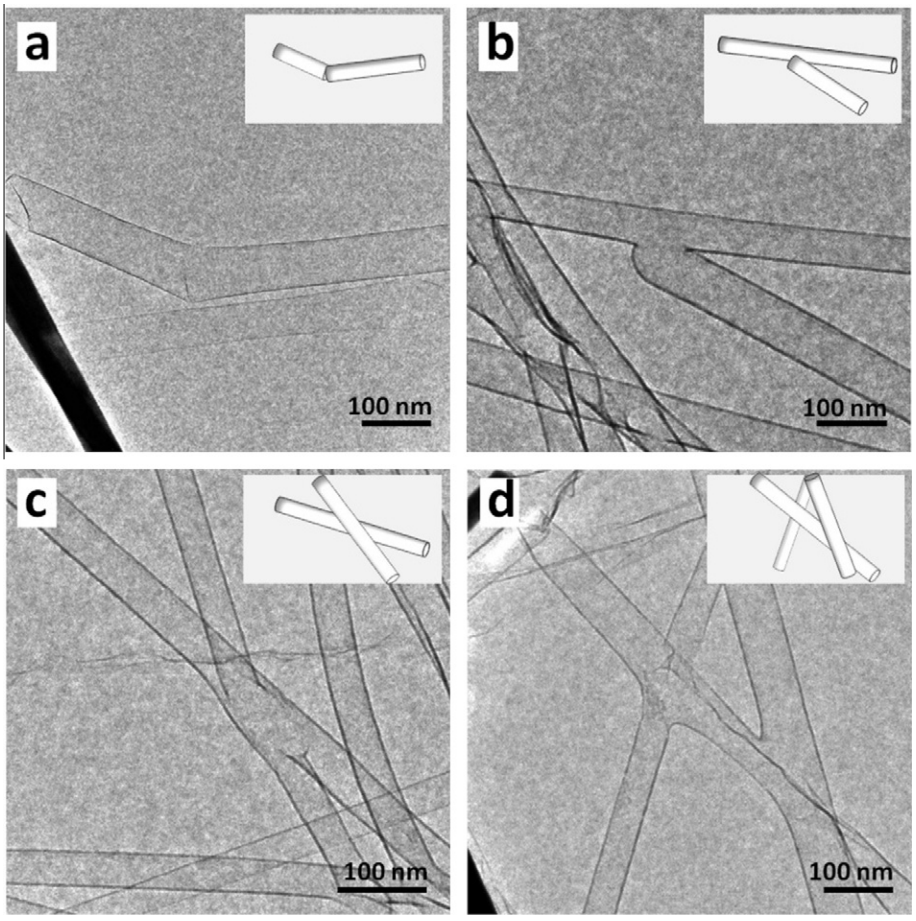

Fig. 4 – Formation of diverse seamless CTS-based structures: (a) a head-to-head connection, (b) a Y-shape connection, (c) a X-shape connection and (d) complex connections. Some weak points of the thin CTSs are unexpectedly damaged during extraction of the molten Ag nanowires. The insets show the schematic constructions of the Ag nanowire templates.

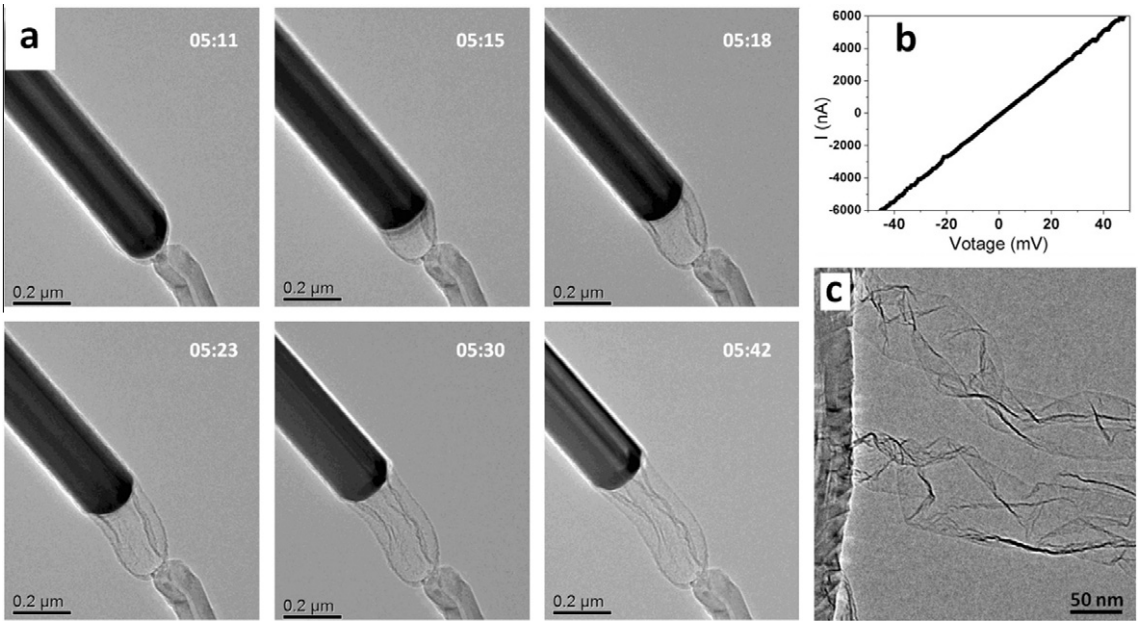

Fig. 5 – (a) An image sequence of extraction of a Ag nanowire by Joule heating under a large bias. The upper electrode is a Ag nanowire covered by amorphous carbon shell while the lower electrode is a commercial MWCNT adhered on a tungsten tip. (b) A measured I-V curve of the formed graphitized CTS in (a). (c) Graphene/graphite sheets formed by extraction of a Ag nanowire covered with thin amorphous carbon sheath under a large bias.

structural damage as shown here the shrinkage in radial direction of the formed nanotube. However, the large current could highly improve the crystal quality of the formed CTS [42]. Fig. 5(b) shows the measured I-V curve of the CTS formed in Fig. 5(a). The excellent conductivity indicates that the initial amorphous structure (which is almost insulated initially) should change into graphitized (See Supplementary for details). Besides, if the deposited carbon layer is very thin (e.g. carbon deposition on spot size 6 only for 5 min with estimated shell thickness of 2 nm), the carbon sheath could no longer bear the large current and usually graphene/graphite sheets are obtained instead of CTSs, as shown in Fig. 5(c).

The mechanical property of the formed CTSs is of great importance to their practical applications. Since the well graphitized CTSs are expected to have outstanding mechanical strength, we here demonstrate the ability of controllable pruning and transportation of Te nanowires by the formed graphitized CTS. Fig. 6(a) shows the video frames of breaking and manipulation of a Te nanowire (see Supplementary video S2). When the Te nanowire is held by the CTS, it is feasible to tailor the Te nanowire by simply moving the tip transversely. The structure of the CTS is well conserved during the nanomanipulation, demonstrating the good mechanical property of the fabricated graphitized CTS.

Since carbon deposition is induced by electron beam irradiation, the geometry of the formed CTSs can therefore be well controlled by precise manipulation of the electron beam. For a large homogeneous electron beam spot, the CTSs are highly uniform. When the electron beam is converged to a small spot, carbon deposition is almost confined inside the beam region and unique tubular structures can be achieved. One may doubt about the geometric symmetry and structural integrity of the formed CTSs since the carbon sheath is electron beam-induced deposited. To identify the spatial structure of the formed CTSs, a Ag nanowire is transferred to a movable tip fixed onto the STM-TEM platform. Carbon sheath is deposited with a convergent electron beam to form a pearl-like thick carbon shell on the Ag nanowire surface. After extracting the Ag by Joule heating, the CTS is spatially characterized and confirmed to be well symmetric tubular shape, as shown in Fig. 6(b) and (c). The CTS exhibits porous structure due to the large current loaded to melt and extract the template Ag nanowire. Nevertheless, it intuitively shows that the carbon sheath is deposited isotropically around the nanowire surface and the cross section of the formed carbon shell structure is obviously symmetric.

4. Summary

A method for the fabrication of CTSs by electron beam-induced carbon deposition with metal nanowires/nanotubes as templates has been presented. The formed carbon tubes show uniform features with designable lengths, diameters and wall thicknesses. Seamless CTS-based structures have been fabricated with multi-type joints using well constructed Ag nanowires as templates. The seamless joints may have practical applications in nanofluidics and nanodevices. Furthermore, the structural features of the fabricated CTSs have been investigated and discussed. By thermal annealing or Joule heating, the CTSs can be well graphitized. The graphitized CTSs show excellent mechanical properties which have been demonstrated by precise manipulation of a Te nanowire.

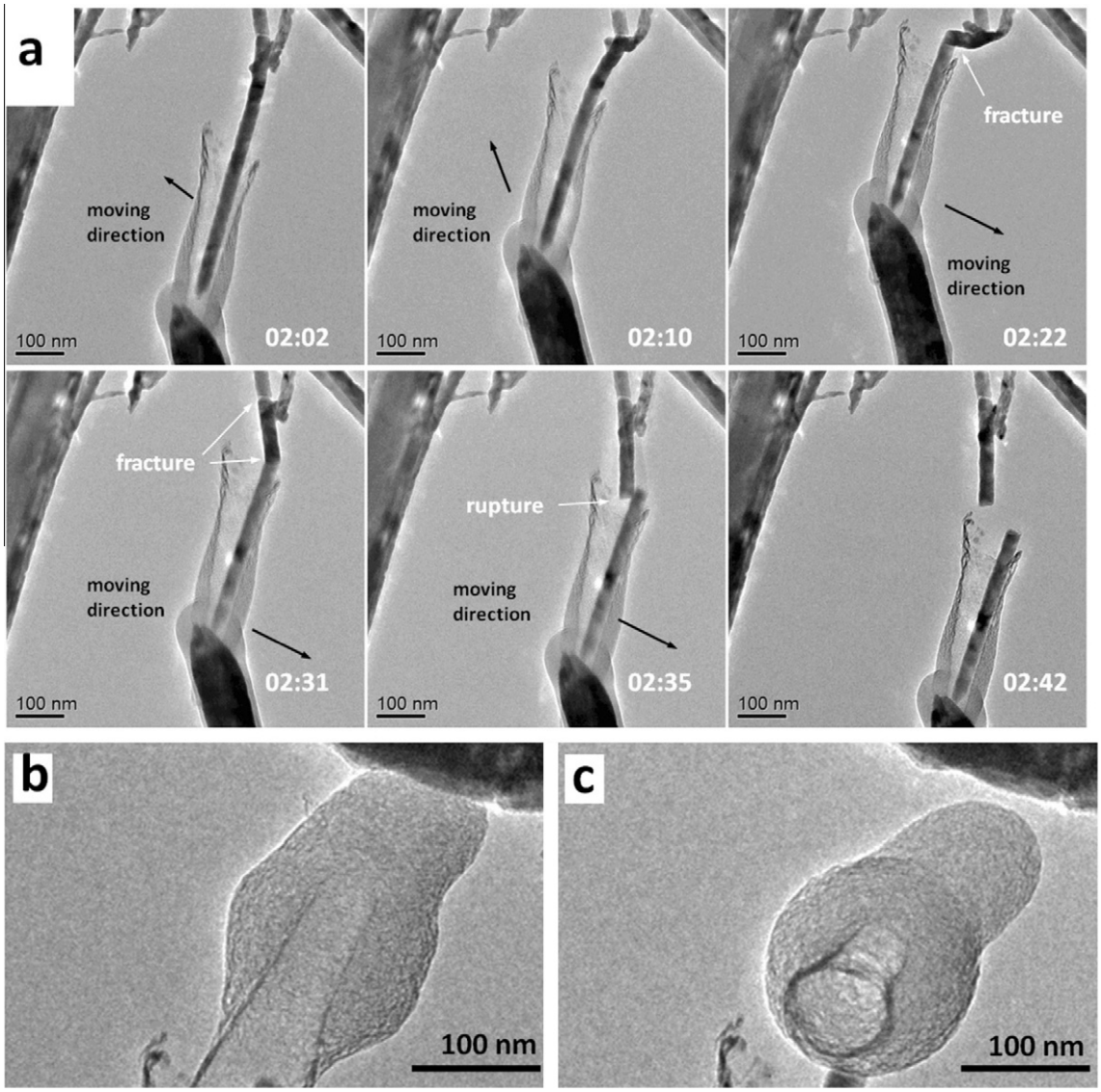

Fig. 6 – (a) An image sequence of breaking and transportation of a Te nanowire by a graphitized CTS. The structure of the CTS retains well, indicating its excellent mechanical property. The black arrows indicate the moving direction of the CTS-decorated tungsten tip. (b) Part of a very thick CTS fabricated by a long period of carbon deposition with a convergent electron beam on spot size 9. The CTS is electrically burned out to characterize its spatial structure. (c) The cross-section image of the CTS.

Acknowledgments

This work was supported by the National Basic Research Program of China (Grant No. 2011CB707601 and No. 2009CB623702), the National Natural Science Foundation of China (Nos. 51071044, 60976003, 61006011 and 61106055), the Natural Science Foundation of Jiangsu Province (No. BK2011592), Specialized Research Fund for the Doctoral Program of Higher Education (Nos. 20100092120021 and 20100092110014) Program for New Century Excellent Talents in University (No. NCEF-09-0293) and Open Research Fund of State Key Laboratory of Bioelectronics. The authors would like to thank Dr. Kaiming Liao in Nanjing University for providing the Te nanowires and nanotubes.

Appendix A. Supplementary data

Supplementary data associated with this article can be found, in the online version, at doi:10.1016/j.carbon.2012.02.051.

REFERENCES

[1] Iijima S. Helical microtubules of graphitic carbon. Nature 1991;354(6348):56–8.
[2] Lee SW, Park SJ, Campbell EEB, Park YW. A fast and low-power microelectromechanical system-based non-volatile memory device. Nat Commun 2011;2:220.

[3] Fan DL, Zhu FQ, Cammarata RC, Chien CL. Electric tweezers. Nano Today 2011;6(4):339–54.
[4] Noy A, Park HG, Fornasiero F, Holt JK, Grigoropoulos CP, Bakajin O. Nanofluidics in carbon nanotubes. Nano Today 2007;2(6):22–9.
[5] Gao YH, Bando Y. Carbon nanothermometer containing gallium – Gallium's macroscopic properties are retained on a miniature scale in this nanodevice. Nature 2002;415(6872):599.
[6] Liu ZW, Bando Y, Mitome M, Zhan JH. Unusual freezing and melting of gallium encapsulated in carbon nanotubes. Phys Rev Lett 2004;93(9):095504.
[7] Singhal R, Bhattacharyya S, Orynbayeva Z, Vitol E, Friedman G, Gogotsi Y. Small diameter carbon nanopipettes. Nanotechnology 2010;21(1):015304.
[8] Collins PG, Bradley K, Ishigami M, Zettl A. Extreme oxygen sensitivity of electronic properties of carbon nanotubes. Science 2000;287(5459):1801–4.
[9] Kong J, Franklin NR, Zhou CW, Chapline MG, Peng S, Cho KJ, et al. Nanotube molecular wires as chemical sensors. Science 2000;287(5453):622–5.
[10] Fennimore AM, Yuzvinsky TD, Han WQ, Fuhrer MS, Cumings J, Zettl A. Rotational actuators based on carbon nanotubes. Nature 2003;424(6947):408–10.
[11] Liu HT, He J, Tang JY, Liu H, Pang P, Cao D, et al. Translocation of single-stranded DNA through single-walled carbon nanotubes. Science 2010;327(5961):64–7.
[12] Chen X, Kis A, Zettl A, Bertozzi CR. A cell nanoinjector based on carbon nanotubes. P Natl Acad Sci USA 2007;104(20):8218–22.
[13] Freedman JR, Mattia D, Korneva G, Gogotsi Y, Friedman G, Fontecchio AK. Magnetically assembled carbon nanotube tipped pipettes. Appl Phys Lett 2007;90(10):103108.
[14] Wang J, Chen G, Chatrathi MP, Musameh M. Capillary electrophoresis microchip with a carbon nanotube-modified electrochemical detector. Anal Chem 2004;76(2):298–302.
[15] Banhart F, Li JX, Terrones M. Cutting single-walled carbon nanotubes with an electron beam: evidence for atom migration inside nanotubes. Small 2005;1(10):953–6.
[16] Li JX, Banhart F. The engineering of hot carbon nanotubes with a focused electron beam. Nano Lett 2004;4(6):1143–6.
[17] Terrones M, Banhart F, Grobert N, Charlier JC, Terrones H, Ajayan PM. Molecular junctions by joining single-walled carbon nanotubes. Phys Rev Lett 2002;89(7):075505.
[18] Terrones M, Terrones H, Banhart F, Charlier JC, Ajayan PM. Coalescence of single-walled carbon nanotubes. Science 2000;288(5469):1226–9.
[19] Wang MS, Wang JY, Chen Q, Peng LM. Fabrication and electrical and mechanical properties of carbon nanotube interconnections. Adv Funct Mater 2005;15(11):1825–31.
[20] Rodriguez-Manzo JA, Wang MS, Banhart F, Bando Y, Golberg D. Multibranched junctions of carbon nanotubes via cobalt particles. Adv Mater 2009;21(44):4477–82.
[21] Jin CH, Suenaga K, Iijima S. Plumbing carbon nanotubes. Nat Nanotechnol 2008;3(1):17–21.
[22] Harris PJF. Carbon nanotube science: synthesis properties and applications. 1st ed. Beijing: Cambridge: University Press; 2010.
[23] Goldberger J, Fan R, Yang PD. Inorganic nanotubes: a novel platform for nanofluidics. Accounts Chem Res 2006;39(4):239–48.
[24] Goldberger J, He RR, Zhang YF, Lee SW, Yan HQ, Choi HJ, et al. Single-crystal gallium nitride nanotubes. Nature 2003;422(6932):599–602.
[25] Sun YG, Xia YN. Multiple-walled nanotubes made of metals. Adv Mater 2004;16(3):264–8.
[26] Hu JQ, Bando Y, Liu ZW, Zhan JH, Golberg D, Sekiguchi T. Synthesis of crystalline silicon tubular nanostructures with ZnS nanowires as removable templates. Angew Chem Int Edit 2004;43(1):63–6.
[27] Yin LW, Bando Y, Zhan JH, Li MS, Golberg D. Self-assembled highly faceted wurtzite-type ZnS single-crystalline nanotubes with hexagonal cross-sections. Adv Mater 2005;17(16):1972–7.
[28] Li YB, Bando Y, Golberg D. Indium-assisted growth of aligned ultra-long silica nanotubes. Adv Mater 2004;16(1):37–40.
[29] Sun YG, Xia YN. Large-scale synthesis of uniform silver nanowires through a soft, self-seeding, polyol process. Adv Mater 2002;14(11):833–7.
[30] Xia YN, Xiong YJ, Lim B, Skrabalak SE. Shape-controlled synthesis of metal nanocrystals: simple chemistry meets complex physics. Angew Chem Int Edit 2009;48(1):60–103.
[31] Lu QY, Gao F, Komarneni S. A green chemical approach to the synthesis of tellurium nanowires. Langmuir 2005;21(13):6002–5.
[32] Koops HWP, Kretz J, Rudolph M, Weber M, Dahm G, Lee KL. Characterization and application of materials grown by electron-beam-induced deposition. Jpn J Appl Phys 1 1994;33(12B):7099–107.
[33] Jin CH, Wang JY, Chen Q, Peng LM. In situ fabrication and graphitization of amorphous carbon nanowires and their electrical properties. J Phys Chem B 2006;110(11):5423–8.
[34] Khalavka Y, Ohm C, Sun L, Banhart F, Sönnichsen C. Enhanced thermal stability of gold and silver nanorods by thin surface layers. J Phys Chem C 2007;111(35):12886–9.
[35] Huang JY, Chen S, Ren ZF, Chen G, Dresselhaus MS. Real-time observation of tubule formation from amorphous carbon nanowires under high-bias Joule heating. Nano Lett 2006;6(8):1699–705.
[36] Wang MS, Golberg D, Bando Y. Interface dynamic behavior between a carbon nanotube and metal electrode. Adv Mater 2010;22(1):93–8.
[37] He LB, Xie B, Song FQ, Xu CH, Zhou JF, Han M. Size controlled synthesis of semiconductor nanocrystals in a continuous-flow mode micro capillary reactor. Eur Phys J D 2009;52(1-3):15–8.
[38] Yen BKH, Stott NE, Jensen KF, Bawendi MG. A continuous-flow microcapillary reactor for the preparation of a size series of CdSe nanocrystals. Adv Mater 2003;15(21):1858–62.
[39] Banhart F, Hernández E, Terrones M. Extreme superheating and supercooling of encapsulated metals in fullerene like shells. Phys Rev Lett 2003;90(18).
[40] Regan BC, Aloni S, Ritchie RO, Dahmen U, Zettl A. Carbon nanotubes as nanoscale mass conveyors. Nature 2004;428(6986):924–7.
[41] Zhao JO, Huang JQ, Wei F, Zhu J. Mass transportation mechanism in electric-biased carbon nanotubes. Nano Lett 2010;10(11):4309–15.
[42] Chen S, Huang JY, Wang Z, Kempa K, Chen G, Ren ZF. High-bias-induced structure and the corresponding electronic property changes in carbon nanotubes. Appl Phys Lett 2005;87(26):263107.